

Strategies for reducing frequency scatter in large arrays of superconducting resonators

J. Li¹, P. S. Barry¹, Z. Pan¹, C. Albert²,
T. Cecil¹, C. L. Chang^{1,2,3}, K. Dibert²,
M. Lisovenko¹, V. Yefremenko¹,

the date of receipt and acceptance should be inserted later

Abstract Superconducting resonators are now found in a broad range of applications that require high-fidelity measurement of low-energy signals. A common feature across almost all of these applications is the need for increased numbers of resonators to further improve sensitivity, and the ability to read out large numbers of resonators without the need for additional cryogenic complexity is a primary motivation. One of the major limitations of current resonator arrays is the observed scatter in the resonator frequencies when compared to the initial design. Here we present recent progress toward identifying one of the dominant underlying causes of resonator scatter, inductor line width fluctuation. We designed and fabricated an array of lumped-element resonators with inductor line width changing from $1.8\mu\text{m}$ to $2.2\mu\text{m}$ in step of $0.1\mu\text{m}$ defined with electron-beam lithography to probe and quantify the systematic variation of resonance frequency across a 6-inch wafer. The resonators showed a linear frequency shift of $\approx 20\text{MHz}$ (140FWHM) and 30MHz (214FWHM), respectively, as they are connected to two different capacitors. This linear relationship matches our theoretical prediction. The widely used MLA photon lithography facility for MKID fabrication has a resolution on the order of 600nm , which could cause frequency fluctuation on the order of 100MHz or 710FWHM.

Keywords mKIDS, frequency scatter, lumped inductor line width variation, e-beam lithography

1 Introduction

Superconducting microwave resonators have been extensively applied as detectors for high sensitivity sensing of excitations such as charge [1, 2, 3] and photons [4,

¹Argonne National Laboratory, 9700 South Cass Avenue., Argonne, IL, 60439, USA

²Dept. of Astronomy & Astrophysics, U. Chicago, 5640 South Ellis Avenue, Chicago, IL, 60637, USA

³Kavli Institute for Cosmological Physics, U. Chicago, 5640 South Ellis Avenue, Chicago, IL, 60637, USA

5] due to their simple fabrication process and frequency domain multiplexing capability. Among the various types of superconducting resonator-based detectors, Microwave Kinetic Inductance Detectors (MKIDs) [6, 7], one of the most popular low-temperature superconducting resonator detectors, have found broad applications [8, 9, 10, 11, 12, 13]. With over a decade of development effort, arrays of MKIDs have evolved to thousands [14, 15] of detectors per wafer with improved detector sensitivity. However, scatter in resonator frequency placement, where the fabricated resonance frequencies are shifted from their designed values, has become a limiting issue for large array productivity. Various parameters could contribute to this fluctuation such as non-uniformity in the critical temperature (T_c) and film thickness, non-uniformity in lithographic processing, and non-uniform etch profiles across the wafer.

One solution for mitigating frequency fluctuations is capacitor trimming [16], a method that improves the MKID frequency distribution at the cost of introducing additional steps. Another approach is to improve MKID materials and fabrication to improve resonator frequency placement, though this approach requires detailed studies to understand the fundamental parameters that result in scatter of the resonator frequency. This paper is an initial investigation along this direction, and studies how geometric variations in resonator fabrication contribute to frequency scatter. Our work is motivated in part by results from our recent MKIDs fabrication where we observed significant line width variation of up to 2 μm for 4 μm -wide features across a 6 inch wafer. This line width variation would significantly change the inductance of our lumped element inductor since the inductance is a strong function of line width. To investigate the impact of the line width variation on frequency placement, we carried out a study using electron beam (e-beam) lithography to fabricate resonators with line widths varying in steps of 100 nm, and evaluated their resonance frequency placement as a function of the line width.

2 Modeling the meander inductance

To develop some intuition about the relationship between changes in linewidth and the resonator frequency, we use an equation for meander inductance on PCB [17]:

$$L_m = \beta \cdot w^\alpha \quad (1)$$

with w the width of the meander strip. Inductance change ΔL_m due to small line width change Δw can be approximated by Taylor expansion around w :

$$\Delta L_m / L_m = \alpha \Delta w / w. \quad (2)$$

Similarly the kinetic inductance change ΔL_K due to line width variation Δw is:

$$\frac{\Delta L_K}{L_K} = -\frac{\Delta w}{w}, \quad (3)$$

where we have used kinetic inductance equation from reference [18].

The corresponding shift in resonator frequency Δf_o is then

$$f_o + \Delta f_o = \frac{1/2\pi}{\sqrt{(L + \Delta L)C}} \quad (4)$$

$$= \frac{1/2\pi}{\sqrt{LC}} \left(1 - \frac{1}{2} \frac{\Delta L}{L} \right) \quad (5)$$

$$= f_o - \frac{1}{2} f_o \frac{\Delta L}{L} \quad (6)$$

and fractional frequency shift

$$\frac{\Delta f_o}{f_o} = -\frac{1}{2} \frac{\Delta L}{L} \quad (7)$$

$$= \frac{1}{2} \left(\alpha \frac{L_m}{L_K + L_m} + \frac{L_K}{L_K + L_m} \right) \frac{\Delta w}{w} \quad (8)$$

We carry out a more detailed model of our resonators by using a Sonnet simulation of our lumped element resonators where we change the inductor width from 1.5 to 2.5 μm in steps of 0.5 μm . Figure 1 shows the results of our simulations for each of our two circuit capacitor designs (see Sec. 3).

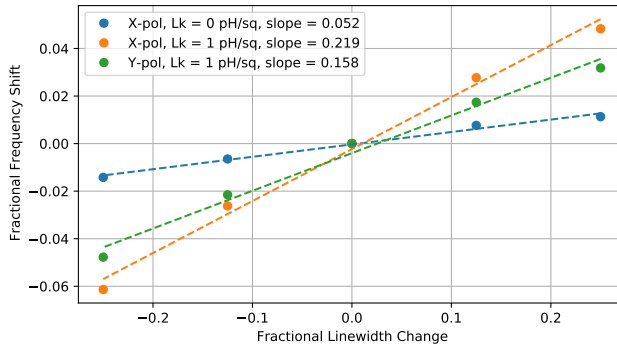


Fig. 1: Simulated fractional resonant frequency shift $\Delta f_o/f_o$ versus fractional line width variation $\Delta w/w$ for “X-pol” and “Y-pol” resonators. Inductor line widths were varied from 1.5 to 2.5 μm in steps of 0.25 μm . L_K is the kinetic inductance of the superconducting thin film in the simulation.

3 Test resonator design

To empirically study the impact of resonator geometry on frequency placement, we designed a test device comprised of five nearly identical lumped element resonators with varying inductor linewidth. In our design (see Fig. 2), we have five pixels, with each pixel having one “X-pol” resonator and a “Y-pol” resonator. All of the “X-pol” (“Y-pol”) resonators have the same circuit capacitor design, C_x (C_y), and the inductor width for both resonators is varied from 1.8 to 2.2 μm in steps of 0.1 μm across the five pixels. With this configuration we expect two groups of resonances corresponding to the two circuit capacitor designs, C_x and C_y . Within each group, we expect to have five linearly distributed resonances corresponding to the five different inductor widths.

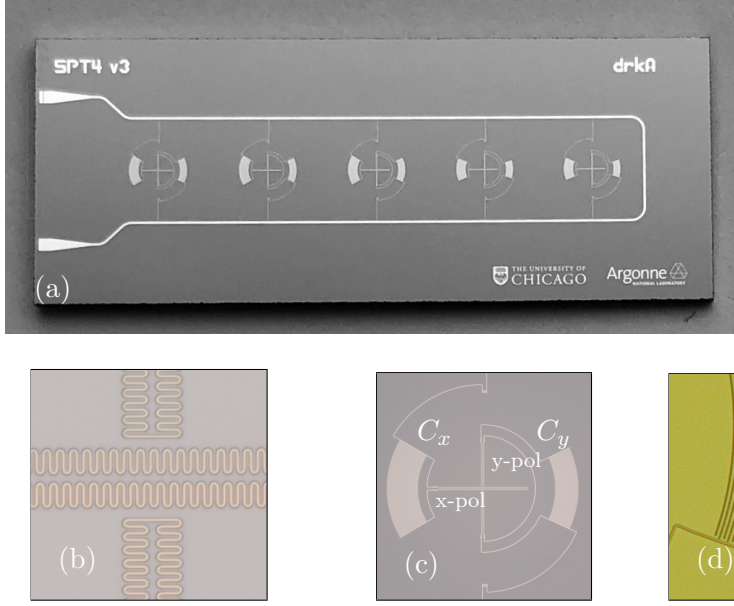


Fig. 2: Images of the designed chip and components. (a) image of chip A which has five pixels and each pixel has two resonator that we name them X and Y because of the orthogonal directional of the two inductors. (b) zoom-in of the meander inductors. (c) zoom-in of the middle pixel. Left inter digital capacitor C_x is connected to the horizontal (X) meander inductor and the right inter digital capacitor C_y is connected to the vertical (Y) meander inductor. (d) zoom in of inter digital capacitor C_y .

4 Fabrication

Our devices were fabricated on a single silicon wafer, which minimizes the impact from comparing materials from different depositions. To achieve the required 100 nm linewidth resolution, the resonators were patterned using ebeam writing with the highest resolution of 10 nm. Details of the fabrication process are:

The bare wafer was vacuum baked in 120°C for six minutes for removing moisture. Ebeam resist of PMMA 950 A4 was spincoated at a speed of 4000rpm for 40 seconds and then baked at 180°C for 4 minutes afterward. The inductor, capacitor, and connection lines are on a single layer and were written with a dose of $720\mu\text{C}/\text{cm}^2$. The feed-through lines as well as the contact pads are on another layer and written with a dose of $800\mu\text{C}/\text{cm}^2$. Proximity effect correction effectively lowers the dose for large structures, and the dose is increased purposely to compensate for it. After pattern writing, the wafer was developed with MIBK and IPA with a ratio of 1:3 for 40 seconds and rinsed in IPA for 10 seconds.

After development a 20 seconds oxygen descum process was applied to remove leftover ebeam resist. Then, a 30 nm thick Al film was deposited via DC magnetron sputtering at a base pressure of $1.7\text{E}-8\text{mBar}$. The final processing step was an overnight soak in acetone for lift-off.

We chose the two tested chips near the center of the wafer to minimize film thickness non-uniformity across the two chips. During fabrication, one of the ca-

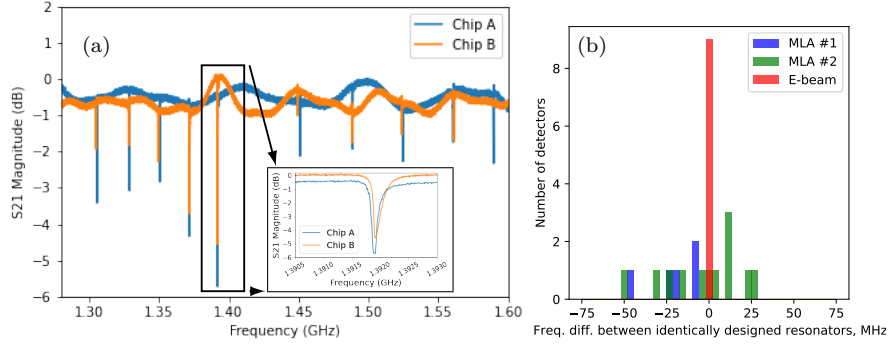


Fig. 3: **(a)** Tested resonator frequencies as a function of inductor line width change. Blue traces is for chip A, and orange trace is for chip B. The inset is zoomed in to the two resonances from chips A and B around 1.3917GHz. An offset of 15 KHz is observed. **(b)** Resonance scatter estimated by comparing the measured frequency for identically designed resonators. Devices fabricated using ebeam lithography with lift-off have scatter <1 MHz, consistent with the 10 nm resolution and our measured geometric dependence. Two other chips (MLA#1 and MLA#2) that were fabricated using Direct Write lithography and wet etching exhibit much larger frequency scatter.

pacitors on one of our devices (chip B) had a liftoff issue and was discarded from our measurements. This only impacted one single resonator.

5 Test results

We tested two chips (chip A and chip B) in a dilution refrigerator with a base temperature of 10 mK. The input lines have ≈ 70 dB attenuation. The output signal is amplified with a HEMT amplifier with a gain of around 40 dB. A superconducting coaxial cable is used between the output of the sample box and the HEMT amplifier to minimize signal loss. The resonances are scanned with a standard S_{21} measurement of VNA.

Figure 3(a) shows the measured resonances for both chip A and B. The trace for chip A shows ten resonances with the lower (higher) frequency resonances corresponding to the resonators with the “Y-pol” (“X-pol”) capacitor design. Within each group, the resonances differ due to the varying inductor linewidth. In Fig. 4, we plot the measured fractional frequency shift, $\Delta f_o/f_o$, versus the change in inductor linewidth, Δw . Our data exhibits a clear linear relationship, as predicted by Eq.(8), with a slope that is consistent with predictions from our simulations.

We estimate the frequency scatter from our ebeam process by comparing the frequencies for identically designed resonators. We find the largest scatter is ~ 1 MHz, which is consistent with the 10 nm ebeam resolution and our measured dependence of inductance on linewidth. To give a sense of the importance of linewidth control, we compare our results with a similar measurement of fre-

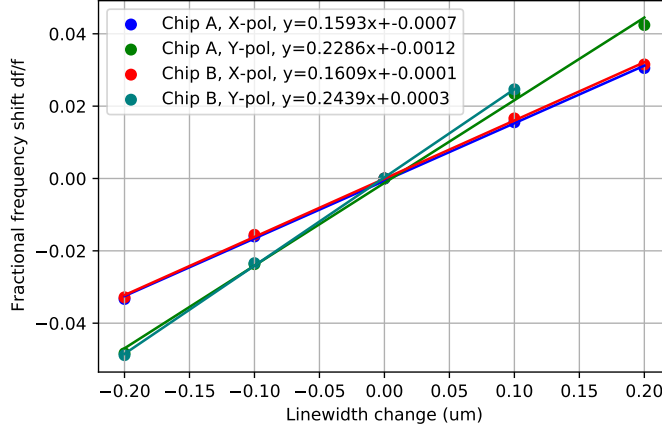


Fig. 4: $\Delta f_o/f_o$ vs. Δw for all the resonators of both chip A and B. “X-pol” stands for resonators that use the C_x capacitor design and “Y-pol” stands for resonators using the C_y capacitor design.

quency scatter for two other sets of resonators that were patterned using Direct Write optical lithography and wet etching (see Fig. 3).

6 conclusion

We have demonstrated the impact of meander linewidth variation on the frequency scatter of lump element resonators. Our results are in good agreement with our simulations and show that control of resonator geometry can be a significant contributor to frequency scatter in large arrays of MKIDs.

Acknowledgements Work at Argonne, including use of the Center for Nanoscale Materials, an Office of Science user facility, was supported by the U.S. Department of Energy, Office of Science, Office of Basic Energy Sciences and Office of High Energy Physics, under Contract No. DE-AC02-06CH11357. Zhaodi Pan is supported by ANL under award LDRD-2021-0186

References

1. R. J. Schoelkopf, P. Wahlgren, A. A. Kozhevnikov, P. Delsing, and D. E. Prober. The radio-frequency single-electron transistor (rf-set): A fast and ultrasensitive electrometer. *Science*, 280(5367):1238–1242, 1998.
2. B. L. Brock, Juliang Li, S. Kanhirathingal, B. Thyagarajan, M. P. Blencowe, and A. J. Rimberg. A fast and ultrasensitive electrometer operating at the single-photon level, 2021.
3. L. Tosi, D. Vion, and H. le Sueur. Design of a cooper-pair box electrometer for application to solid-state and astroparticle physics. *Phys. Rev. Applied*, 11:054072, May 2019.
4. M. D. Shaw, J. Bueno, P. Day, C. M. Bradford, and P. M. Echternach. Quantum capacitance detector: A pair-breaking radiation detector based on the single cooper-pair box. *Phys. Rev. B*, 79:144511, Apr 2009.

5. P. M. Echternach, B. J. Pepper, T. Reck, and C. M. Bradford. Single photon detection of 1.5 thz radiation with the quantum capacitance detector. *Nature Astronomy*, 2(1):90–97, Jan 2018.
6. Peter K. Day, Henry G. LeDuc, Benjamin A. Mazin, Anastasios Vayonakis, and Jonas Zmuidzinas. A broadband superconducting detector suitable for use in large arrays. *Nature*, 425:817 EP –, Oct 2003.
7. S. Doyle, P. Mauskopf, J. Naylor, A. Porch, and C. Duncombe. Lumped element kinetic inductance detectors. *Journal of Low Temperature Physics*, 151(1):530–536, Apr 2008.
8. J. Baselmans, S. J. C. Yates, R. Barends, Y. J. Y. Lankwarden, J. R. Gao, H. Hoevers, and T. M. Klapwijk. Noise and sensitivity of aluminum kinetic inductance detectors for sub-mm astronomy. *Journal of Low Temperature Physics*, 151(1):524–529, Apr 2008.
9. J. Hubmayr et al. Photon-noise limited sensitivity in titanium nitride kinetic inductance detectors. *Applied Physics Letters*, 106(7):073505, 2015.
10. Benjamin A. Mazin, Bruce Bumble, Seth R. Meeker, Kieran O’Brien, Sean McHugh, and Eric Langman. A superconducting focal plane array for ultraviolet, optical, and near-infrared astrophysics. *Opt. Express*, 20(2):1503–1511, Jan 2012.
11. D. C. Moore, S. R. Golwala, B. Bumble, B. Cornell, P. K. Day, H. G. LeDuc, and J. Zmuidzinas. Position and energy-resolved particle detection using phonon-mediated microwave kinetic inductance detectors. *Applied Physics Letters*, 100(23):232601, 2012.
12. Sam Rowe et al. A passive terahertz video camera based on lumped element kinetic inductance detectors. *Review of Scientific Instruments*, 87(3):033105, 2016.
13. W. Guo, X. Liu, Y. Wang, Q. Wei, L. F. Wei, J. Hubmayr, J. Fowler, J. Ullom, L. Vale, M. R. Vissers, and J. Gao. Counting near infrared photons with microwave kinetic inductance detectors. *Applied Physics Letters*, 110(21):212601, 2017.
14. J. C. van Eyken, M. J. Strader, A. B. Walter, S. R. Meeker, P. Szypryt, C. Stoughton, K. O’Brien, D. Marsden, N. K. Rice, Y. Lin, and B. A. Mazin. THE ARCONS PIPELINE: DATA REDUCTION FOR MKID ARRAYS. 219(1):14, jul 2015.
15. S. Shu, M. Calvo, S. Leclercq, J. Goupy, A. Monfardini, and E. F. C. Driessen. Prototype high angular resolution lekids for nika2. *Journal of Low Temperature Physics*, 193(3):141–148, Nov 2018.
16. X. Liu, W. Guo, Y. Wang, M. Dai, L. F. Wei, B. Dober, C. M. McKenney, G. C. Hilton, J. Hubmayr, J. E. Austermann, J. N. Ullom, J. Gao, and M. R. Vissers. Superconducting micro-resonator arrays with ideal frequency spacing. *Applied Physics Letters*, 111(25):252601, 2017.
17. Goran Stojanovic and Mirjana Damjanovic. Compact form of expressions for inductance calculation of meander inductors. *Serbian Journal of Electrical Engineering*, 1, 01 2004.
18. Anthony J Annunziata, Daniel F Santavicca, Luigi Frunzio, Gianluigi Catelani, Michael J Rooks, Aviad Frydman, and Daniel E Prober. Tunable superconducting nanoinductors. 21(44):445202, oct 2010.